Available Online: 5 February 2026 DOI: 10.54254/2977-3903/2026.31648

Rethinking critical behavior in sandpile models: the role of long-range connections and local asymmetry

Yiqun Wang

Faculty of Innovation Engineering, Macau University of Science and Technology, Macau, China

ethan07142012@gmail.com

Abstract. The sandpile model, a foundational cellular automaton, is a paradigm for studying self-organized criticality in complex systems. The critical state is characterized by system-wide avalanches whose sizes follow a power-law distribution. However, the exponent of this distribution, which defines the system's universality class, is sensitive to the underlying interaction rules. This study systematically investigates the influence of network topology on self-organized criticality by simulating sandpile models under both open and periodic boundary conditions. We focus on two key modifications to the classical model: the spatial symmetry of local collapse rules and the impact of long-range connections. Our numerical results demonstrate that breaking the spatial symmetry of the toppling neighborhood causes the power-law exponent of the avalanche distribution to shift from -1.0 to approximately -1.3. Furthermore, introducing even a small fraction of long-range connections drives the exponent to approximately -1.5. These findings demonstrate that both local symmetries and global network connectivity can qualitatively alter the critical behavior, inducing a transition between universality classes. Given that long-range correlations are common in many natural and engineered systems, this work provides a crucial understanding of their critical properties and establishes a basis for subsequent research on stochastic complex networks.

Keywords: sandpile models, collapse rules, self-organized criticality

1. Introduction

Complex systems across nature and technology, from the firing of neural networks to the dynamics of financial markets, often exhibit scale-invariant behavior that emerges without the fine-tuning of external parameters. Self-Organized Criticality (SOC) offers a powerful framework for explaining this phenomenon, suggesting that such systems naturally evolve toward a critical state where a small local perturbation can trigger a system-wide cascade, or "avalanche" [1, 2].

The archetypal model for SOC is the cellular automaton introduced by Bak, Tang, and Wiesenfeld (BTW), known as the sandpile model [1]. In its operation, a "grain of sand" is added to a random site on a lattice. As grains accumulate, the local height at a site increases until it surpasses a critical threshold, triggering a "toppling" event where the unstable site sheds particles to its immediate neighbors. This simple, local rule can initiate a chain reaction that propagates across the system, producing avalanches of all sizes. The distribution of these avalanche sizes follows a robust power law, a hallmark of critical behavior analogous to a surprising variety of natural phenomena, including the Gutenberg-Richter law for earthquakes, the frequency of solar flares, and patterns of collective brain activity [3, 4].

The universality class of the BTW model, defined by the exponent of its power-law distribution, has been shown to be remarkably stable for systems built upon symmetric, short-range interactions. Since its inception, the model has become a cornerstone of complex systems science and has been extensively adapted. Researchers have extended it to higher dimensions, implemented it on various lattice types beyond the simple square grid, and explored numerous variations in its toppling rules to better match specific physical systems [5, 6].

Despite this wealth of research, most studies have preserved the core assumptions of local, symmetric connectivity. However, many real-world complex systems, such as distributed sensor networks and message dissemination protocols, feature interactions that are neither strictly local nor perfectly symmetric [7-10]. For example, neural systems possess long-range axonal connections that act as informational shortcuts, and embers carried by wind can spark new fires far from the original flame front. How such topological variations fundamentally alter the properties of SOC is not fully understood and remains an area of active investigation and poses a challenge to applying the simple model to more realistic scenarios [11, 12].

In this paper, we systematically investigate how the critical behavior of the sandpile model is altered by relaxing these two foundational assumptions. Using numerical simulations, we analyze two key scenarios under periodic boundary conditions to ensure translational symmetry and minimize finite-size effects. Our first line of inquiry addresses the impact of breaking the spatial symmetry of the local toppling rules, a feature relevant to systems with inherent anisotropy or directional flows. Our second investigation is motivated by the prevalence of "small-world" phenomena; we quantify the effect of introducing a tunable number of long-range connections, which allow toppling particles to be transported to randomly chosen distant sites. This effectively creates a bridge between purely local dynamics and a mean-field interaction.

We demonstrate that the universality class of the sandpile model is highly sensitive to these modifications. We find that breaking local symmetry shifts the critical exponent of the avalanche size distribution from the canonical value of approximately -1.0 to -1.3. More significantly, the introduction of even a sparse number of long-range connections drives the system into a different, mean-field universality class characterized by an exponent of approximately -1.5. These results underscore the crucial role that network topology plays in shaping the macroscopic dynamics of self-organizing systems.

2. Sandpile model and self-organized criticality

This section introduces the theoretical framework of the sandpile model and Self-Organized Criticality (SOC), detailing the model's mechanics as a cellular automaton, the metrics for avalanche analysis, and the simulation methodologies used in this study.

2.1. Cellular automaton

The sandpile model is a type of Cellular Automaton (CA), a discrete dynamical system defined by a grid of cells, their states, and rules for their evolution [13-15]. In this context, the grid is the lattice of the sandpile, and the state of each cell (or site) is the integer number of sand grains it holds. The evolution is determined by local rules governing how cells interact with their neighbors.

This study considers two standard neighborhood definitions, as shown in Figure. 1:

• The Von Neumann neighborhood, which consists of the four cardinally adjacent cells (up, down, left, right).

• The Moore neighborhood, which includes the four Von Neumann neighbors plus the four diagonally adjacent cells, for a total of eight neighbors.

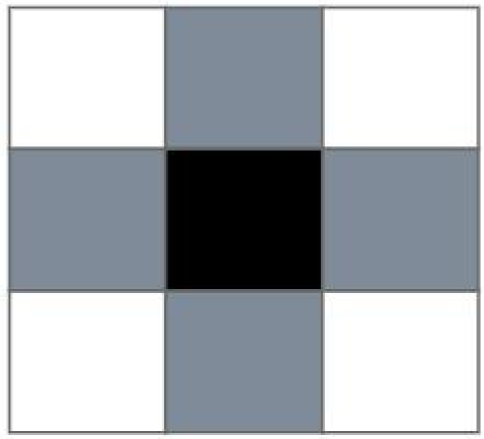

Figure 1. The Von Neumann (left) and Moore (right) neighborhoods. The central black square is the site being considered, and the gray squares are its neighbors

The specific "collapse rule", detailed below, is a local interaction rule based on a cell's state and its defined neighborhood, which gives rise to global, complex behavior [13].

2.2. Sandpile model

The sandpile model is implemented on a 2D integer array representing the lattice. The value of an element at coordinates (i, j) corresponds to the number of sand grains, or height, $z(i, j)$ at that site. A visualization of the system after it has reached a critical state is shown in Figure. 2.

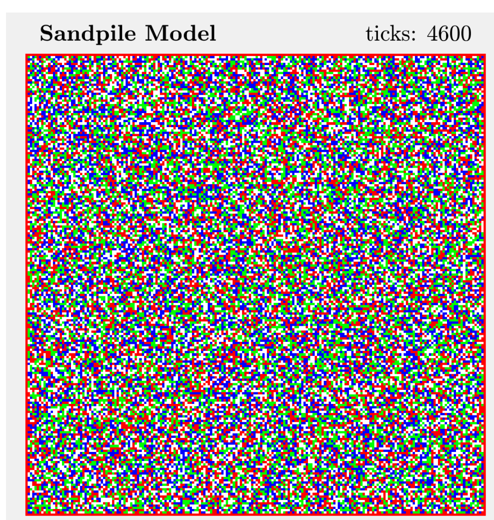

Figure 2. A visualization of the sandpile model in its critical state on a 200 × 200 lattice. Sites are color-coded by height $z(i, j)$

The system is driven by randomly adding a single grain of sand at a time to a site (i_r, j_r) chosen uniformly at random:

$$z(i_r, j_r) \to (i_r, j_r) + 1 \quad (1)$$

Following this addition, the system checks for instabilities. A site (i, j) is considered stable if its height is below a critical threshold, $z(i, j) < z_{cr}$. If one or more sites are unstable, with $z(i, j) > z_{cr}$, a relaxation process (an avalanche) occurs until all sites in the system are once again stable.

2.3. Collapse rule

The relaxation process is governed by the model's collapse rule (also known as the toppling rule). When a site (i, j) becomes unstable, it sheds a fixed number of grains, m , which are distributed one by one to its m designated neighbors. Let the set of m neighbors for site (i, j) be denoted by $N(i, j)$. The rule can be expressed as:

$$Ifz(i,j) > z_{cr} : \begin{cases} z(i,j) \to z(i,j) - m \\ z(i\prime, j\prime) \to z(i\prime, j\prime) + 1, \forall (i\prime, j\prime) \in N(i,j) \end{cases} \quad (2)$$

In this work, the collapse neighborhood $N(i, j)$ may consist of the four nearest neighbors (Von Neumann), eight nearest neighbors (Moore), or other configurations involving long-range connections, as detailed in Section 2.7.

2.4. Avalanche scale

The central analysis of this study focuses on the statistical properties of avalanches. We measure the scale of each avalanche using two distinct metrics:

1. Avalanche Size (s_t): The total number of toppling events that occur during one relaxation cascade.

2. Avalanche Area (s_a): The number of unique sites that topple at least once during the cascade. To calculate this, a helper matrix e of the same dimensions as the system lattice is used. When a site (i, j) topples, the corresponding element $e(i, j)$ is incremented. The avalanche area s_a is the final count of non-zero elements in e .

For each simulation, the frequencies of avalanche sizes are collected into a histogram, which is then normalized to produce a probability distribution for each metric.

2.5. The self-organized critical state

A self-organized critical state describes the condition to which some complex dynamical systems spontaneously evolve without any fine-tuning of system parameters [12]. Once in this state, the system exhibits a high sensitivity to small perturbations, where a minor local event can trigger a response of any size. This critical state is characterized by long-range spatiotemporal correlations and fractal structures [1, 16]. The core of the phenomenon is that the system self-organizes its internal structure (e.g., the slopes on the sandpile) to a point of marginal stability, where it is perpetually susceptible to cascading failures or avalanches [13].

2.6. The power-law distribution

A key signature of a system in a self-organized critical state is that the magnitude of its response events follows a power-law distribution. For a variable s (such as avalanche size), the probability $P(s)$ is given by:

$$P(s) \propto s^{-\tau} \quad (3)$$

where τ is the critical exponent. When plotted on a log-log scale, this relationship appears as a straight line with a slope of - τ :

$$lnP(s) = C - \tau lns \quad (4)$$

In the sandpile model, the distribution of avalanche sizes follows such a law. The value of the exponent τ is a robust quantity that defines the model's universality class. This study investigates how different collapse rules and network structures alter this critical exponent.

2.7. Simulation protocol and analysis

This work investigates the critical behavior of the sandpile model under various topological rules and boundary conditions. All sandpile models were simulated in MATLAB. The system was simulated under two boundary conditions: open, where grains falling off the edge are removed, and periodic, where the lattice edges wrap around to form a torus.

The core of the study involved systematically varying the collapse rules:

• We first established baselines using the classical four-neighbor (Von Neumann) and eight-neighbor (Moore) rules.

• We then investigated the role of spatial symmetry by defining fixed collapse rules where four neighbors are chosen from the eight available Moore sites in both symmetric and asymmetric configurations. Random and random-fixed versions of these rules were also tested.

• To study the influence of interaction range, we varied the size of the square collapse neighborhood from 2 × 2 to 100 × 100.

• Finally, we introduced long-range connections by modifying the four-neighbor rule to allow one, two, three, or all four grains to be transferred to randomly selected sites across the entire lattice.

For each simulation, we collected the distributions of avalanche size (s_t) and area (s_a) and plotted them on a log-log scale. The critical exponent τ was determined by performing a linear fit on the tail of the resulting distribution.

3. Sandpile models under the open boundary condition

3.1. The four-neighbor sandpile model

The canonical sandpile model, often referred to as the Bak-Tang-Wiesenfeld (BTW) model, is defined on a two-dimensional square lattice. Our simulation is conducted on a 200 × 200 lattice with open boundary conditions, where particles toppling from the edges are removed from the system. The state of the system is defined by the number of particles, or height, $z(x_i, y_i)$ at each site (x_i, y_i) .

A site becomes unstable if its height reaches or exceeds a critical threshold, $z_{cr} = 4$. When an unstable site topples, its height is reduced by four, and one particle is distributed to each of its four nearest neighbors in the Von Neumann neighborhood. This deterministic, local toppling rule is applied uniformly to all sites and is described by Equation 5.

$$Ifz(x_i, y_i) \geq 4 \begin{cases} z(x_i, y_i) \to z(x_i, y_i) - 4 \\ z(x_i \pm 1, y_i) \to z(x_i \pm 1, y_i) + 1 \\ z(x_i, y_i \pm 1) \to z(x_i, y_i \pm 1) + 1 \end{cases} \tag{5}$$

To drive the system to its self-organized critical state, we added 200,000 particles sequentially to randomly selected sites. The resulting probability distributions for avalanche events were analyzed. As shown in Figure 3, the distributions for both the avalanche size (total number of topples) and the avalanche area (number of unique sites involved) exhibit power-law behavior. A linear fit on the log-log scale yields a critical exponent of $\alpha \approx -1.06$ for both metrics. This result is consistent with established findings for the BTW model and confirms its placement within a well-defined universality class.

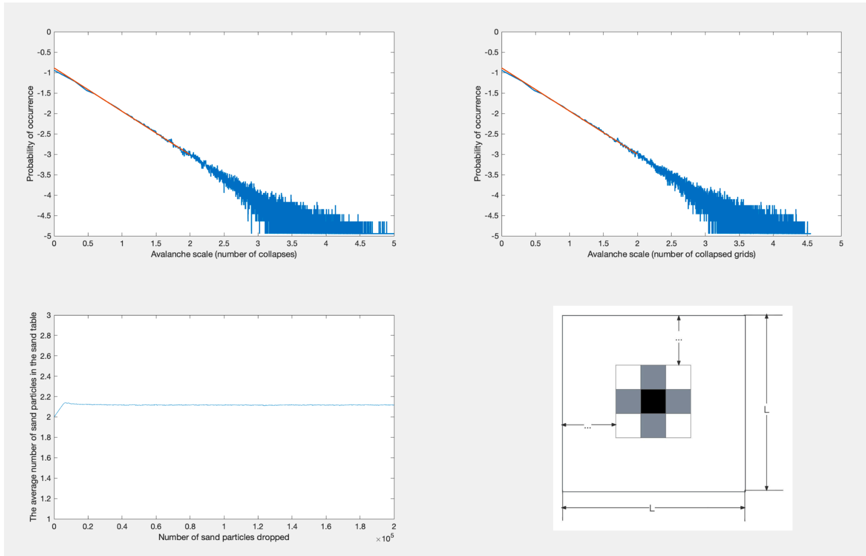

Figure 3. Schematic of the toppling rule for the four-neighbor model

3.2. The eight-neighbor sandpile model

We next investigate a variation of the model by expanding the toppling neighborhood from the four Von Neumann neighbors to the eight surrounding sites defined by the Moore neighborhood. The simulation maintains a fixed network structure and open boundary conditions.

In this configuration, a site is considered unstable when its height $z(x_i, y_i)$ reaches a critical threshold of $z_{cr} = 8$. Upon toppling, the site's height is reduced by eight, and one particle is transferred to each of its eight nearest and next-nearest neighbors. The rule is defined in Equation 6.

$$If z(x_i, y_i) \geq 8 \begin{cases} z(x_i, y_i) \rightarrow z(x_i, y_i) - 8 \\ z(x_i + \delta x, y_i + \delta y) \rightarrow z(x_i + \delta x, y_i + \delta y) + 1, \\ forall \delta x, \delta y \in \{-1, 0, 1\} where (\delta x, \delta x) \neq (0, 0) \end{cases} \tag{6}$$

Following the same simulation procedure on a 200 × 200 lattice with 200,000 particle additions, it is found that this model also reaches a self-organized critical state. The power-law fit of the avalanche distributions (see Figure 4) reveals a critical exponent of α ≈ -1.11 for the avalanche size and α ≈ -1.10 for the avalanche area.

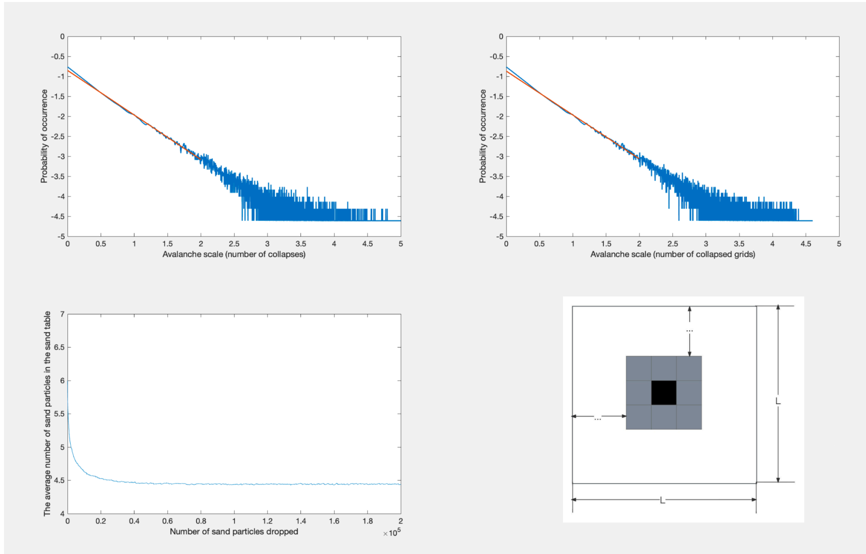

Figure 4. Schematic of the eight-neighbor toppling rule

3.3. Sandpile models with modified toppling structures

To investigate how toppling geometry influences the critical behavior of the sandpile model, we designed and simulated three classes of models with modified toppling rules under open boundary conditions: fixed structures, random-fixed structures, and fully random structures.

3.3.1. Fixed toppling structures

In this class of models, the study explores rules where an unstable site topples to a fixed subset of four neighbors chosen from the eight-site Moore neighborhood. The critical threshold is set to $z_{cr} = 4$. We focus on how the spatial symmetry of the toppling pattern affects the system's critical exponents.

We first examine two toppling patterns that are symmetric with respect to the lattice axes.

Scenario 1: Diagonal Neighbors. The first rule directs particles to the four diagonal neighbors. The toppling rule is given by Equation 7.

$$If z(x_i, y_i) \geq 4 \begin{cases} z(x_i, y_i) \to z(x_i, y_i) - 4 \\ z(x_i \pm 1, y_i \pm 1) \to z(x_i \pm 1, y_i \pm 1) + 1 \\ z(x_i \mp 1, y_i \pm 1) \to z(x_i \mp 1, y_i \pm 1) + 1 \end{cases} \tag{7}$$

As shown in Figure 5, simulation of this model yields a critical exponent of $\alpha \approx$ -1.05 for both avalanche size and area.

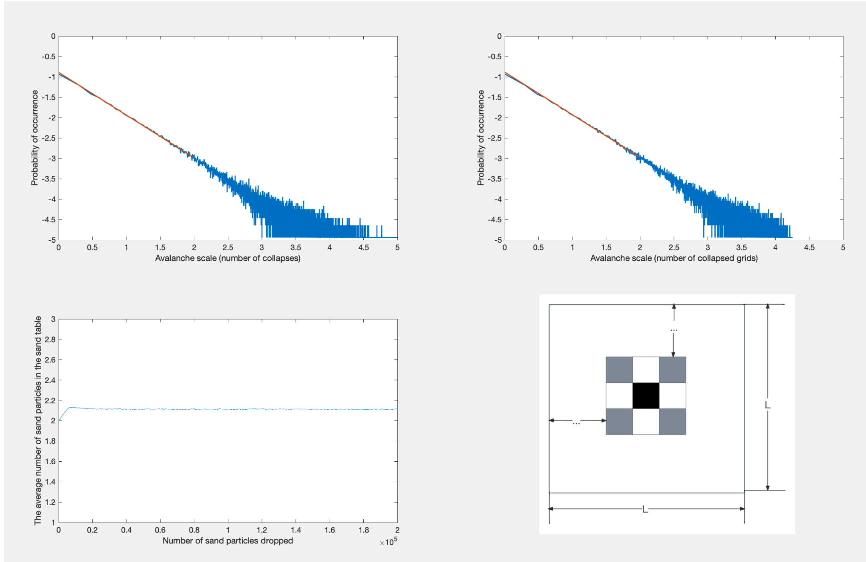

Figure 5. Schematic and avalanche distribution for the first symmetric fixed structure (Scenario 1)

Scenario 2: Mixed Neighbors. The second symmetric rule directs particles to the neighbors at positions relative to the toppling site of $\{(-1,1),(0,-1),(0,1),(1,-1)\}$, defined in Equation 8.

$$If z(x_i, y_i) \geq 4 \begin{cases} z(x_i, y_i) \rightarrow z(x_i, y_i) - 4 \\ z(x_i, y_i \pm 1) \rightarrow z(x_i, y_i \pm 1) + 1 \\ z(x_i \pm 1, y_i \mp 1) \rightarrow z(x_i \pm 1, y_i \mp 1) + 1 \end{cases} \tag{8}$$

This model also results in a critical exponent of $\alpha \approx$ -1.05 for both avalanche metrics, as seen in Figure 6.

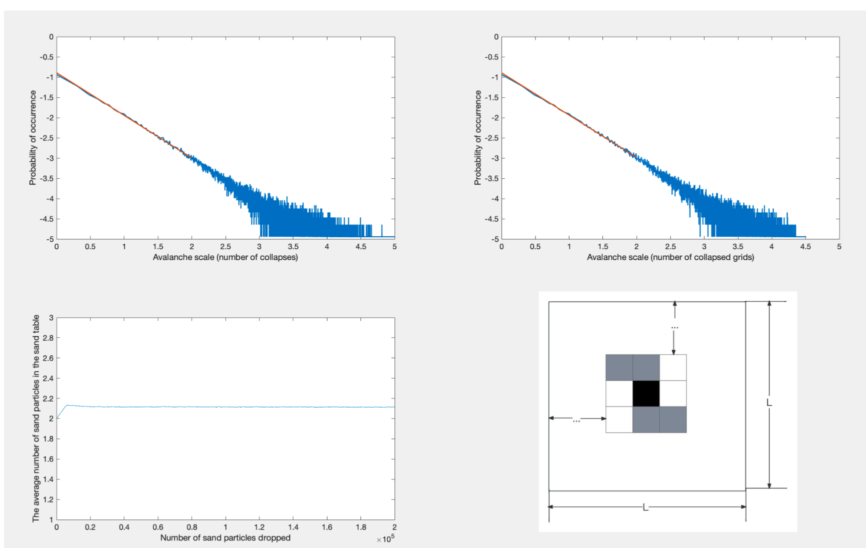

Figure 6. Schematic and avalanche distribution for the second symmetric fixed structure (Scenario 2)

Next, we investigate two toppling patterns that break spatial symmetry.

Scenario 3. The first asymmetric rule (see Equation 9) directs topples to neighbors at $\{(-1,1),(0,-1),(0,1),(1,1)\}$.

$$Ifz(x_i, y_i) \geq 4 \begin{cases} z(x_i, y_i) \rightarrow z(x_i, y_i) - 4 \\ z(x_i, y_i \pm 1) \rightarrow z(x_i, y_i \pm 1) + 1 \\ z(x_i + 1, y_i + 1) \rightarrow z(x_i + 1, y_i + 1) + 1 \\ z(x_i - 1, y_i + 1) \rightarrow z(x_i - 1, y_i + 1) + 1 \end{cases} \tag{9}$$

The simulation (Figure 7) yields exponents of $\alpha \approx$ -1.29 (size) and $\alpha \approx$ -1.30 (area).

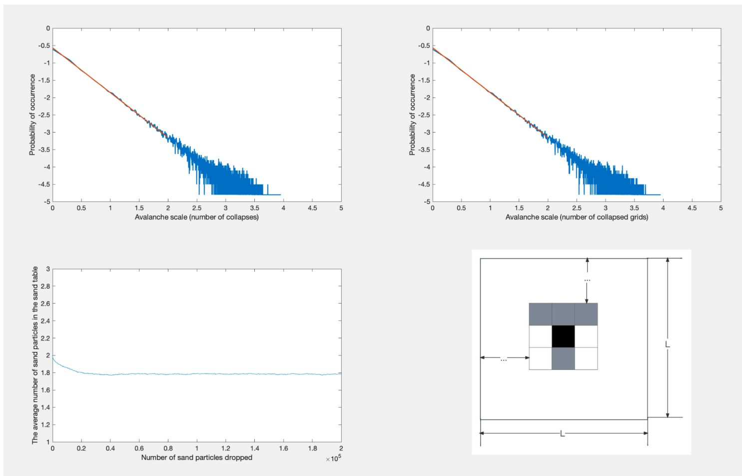

Figure 7. Schematic and avalanche distribution for the first asymmetric fixed structure (Scenario 3)

Scenario 4. The second asymmetric rule (Equation 10) directs topples to neighbors at $\{(-1,-1),(-1,1),(0,-1),(0,1)\}$.

$$Ifz(x_i, y_i) \geq 4 \begin{cases} z(x_i, y_i) \rightarrow z(x_i, y_i) - 4 \\ z(x_i, y_i \pm 1) \rightarrow z(x_i, y_i \pm 1) + 1 \\ z(x_i - 1, y_i \pm 1) \rightarrow z(x_i - 1, y_i \pm 1) + 1 \end{cases} \tag{10}$$

This model (Figure 8) results in a critical exponent of $\alpha \approx$ -1.35 for both metrics.

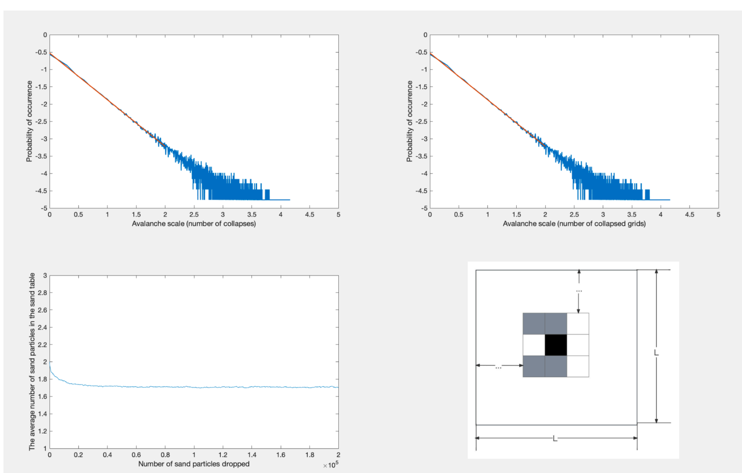

Figure 8. Schematic and avalanche distribution for the second asymmetric fixed structure (Scenario 4)

The results of the four scenarios demonstrate a clear distinction. The two symmetric structures yield a critical exponent $\alpha \approx$ -1.05, which is consistent with the canonical BTW model. In contrast, the two asymmetric structures produce a significantly different exponent, averaging $\alpha \approx$ -1.32. This suggests that while symmetric variations belong to the same universality class as the BTW model, breaking the toppling symmetry is sufficient to define a new universality class.

3.3.2. Random-fixed structure

In this model, we introduce quenched disorder. For each site (x_i, y_i) on the lattice, we randomly pre-select and fix a set of four unique neighbors, N_i , from its Moore neighborhood. This toppling pattern is fixed for the duration of the simulation but varies from site to site. The rule is:

$$Ifz(x_i, y_i) \geq 4 \begin{cases} z(x_i, y_i) \to z(x_i, y_i) - 4 \\ z_j \to z_j + 1, foreachneiguborj \in N_i \end{cases} \quad (11)$$

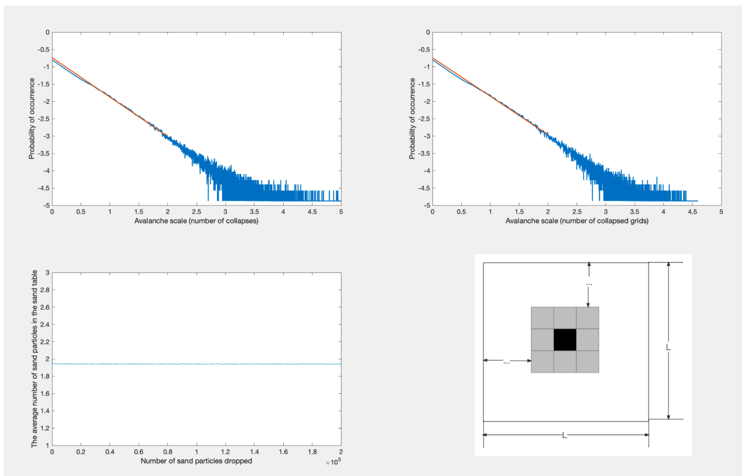

Figure 9. Schematic and avalanche distribution for a single realization of the random-fixed structure model

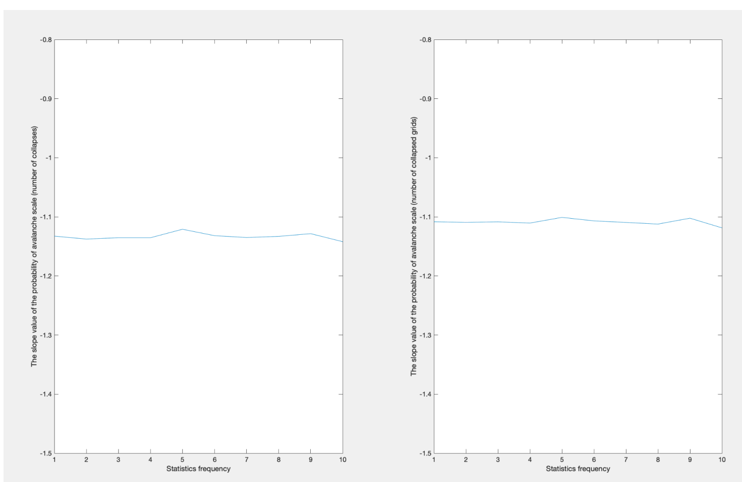

Figure 10. The average critical exponents for ten different realizations of the random-fixed structure model

A single realization of this model is shown in Figure 9. To obtain a more robust statistical result, we generated ten different random-fixed network configurations and ran the full simulation for each. The averaged results (Figure 10) yield a critical exponent for avalanche size of $\alpha \approx$ -1.13 and for an avalanche area of $\alpha \approx$ -1.11.

3.3.3. Random structure

Finally, we consider a fully dynamic random model. In this case, the toppling neighborhood is not quenched but is redefined at every individual toppling event. When a site i becomes unstable, it randomly selects a set, $N_i(t)$, of four unique neighbors from its Moore neighborhood at that moment. The rule can be expressed as:

$$If z_i \geq 4 : \begin{cases} z_j \rightarrow z_j - 4 \\ z_j \rightarrow z_j + 1, \forall j \in N_i(t) \end{cases} \tag{12}$$

This model, shown in Figure 11, yields a critical exponent of α ≈ -1.14 for avalanche size and α ≈ -1.12 for the avalanche area. Interestingly, the exponents for both the random-fixed and the dynamic random models are approximately the average of the exponents from the symmetric (≈ -1.05) and asymmetric (≈ -1.32) fixed-structure cases.

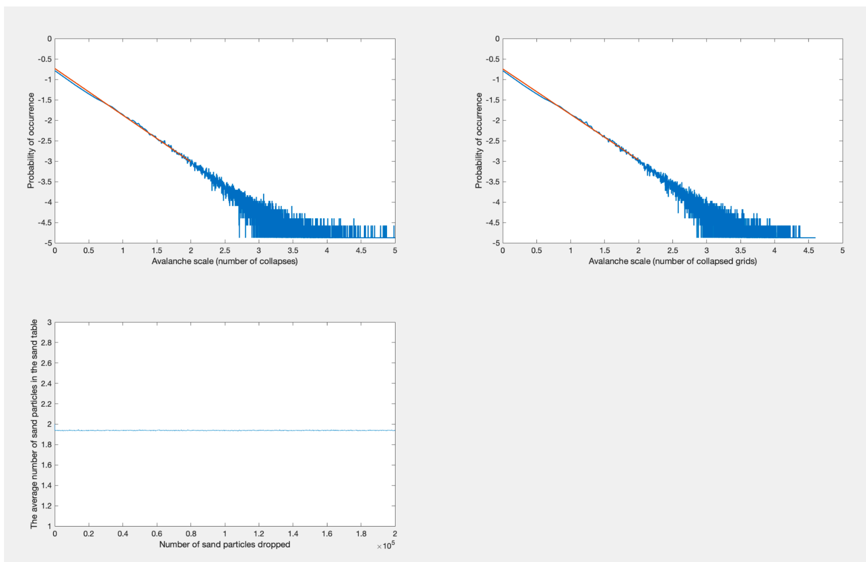

Figure 11. Avalanche distribution for the dynamic random structure model

4. Sandpile models under the periodic boundary condition

4.1. Evaluation under periodic boundary conditions

To isolate the bulk properties of the system and eliminate edge effects, we repeated our analysis using periodic boundary conditions, where the lattice effectively forms a torus. In a conservative system, avalanches can persist indefinitely. To prevent this, a small dissipation mechanism was introduced: for each toppling event, there is a probability $p_d = 4/L$ (where L = 200 is the linear system size) that one of the four grains is removed from the system. If this does not occur, the topple proceeds normally. The following experiments mirror those performed with open boundaries, using a 200×200 lattice driven by 200,000 particle additions.

4.1.1. Fixed toppling structures

We first analyze the four "eight-choose-four" fixed toppling structures, examining the role of spatial symmetry.

Scenario 1: Diagonal Neighbors. The first symmetric rule directs particles to the four diagonal neighbors. This model yields a critical exponent of α ≈ -0.94 for avalanche size and α ≈ -0.93 for the avalanche area, as shown in Figure 12.

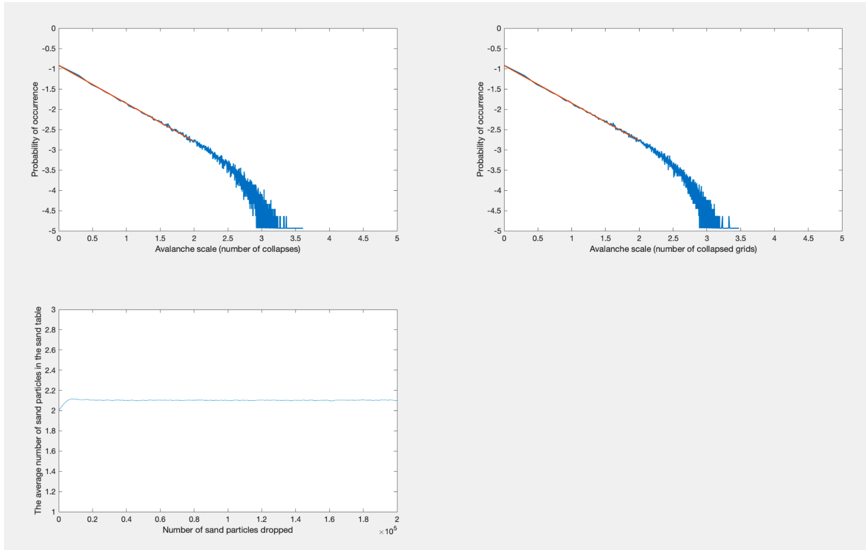

Figure 12. Avalanche size distributions for the diagonal symmetric toppling rule under periodic boundary conditions

Scenario 2: Mixed Neighbors. The second symmetric rule directs particles to the neighbors at relative positions $\{(-1,1),(0,-1),(0,1),(1,-1)\}$. This configuration results in a nearly identical exponent of $\alpha \approx$ -0.93 for both metrics, as shown in Figure 13.

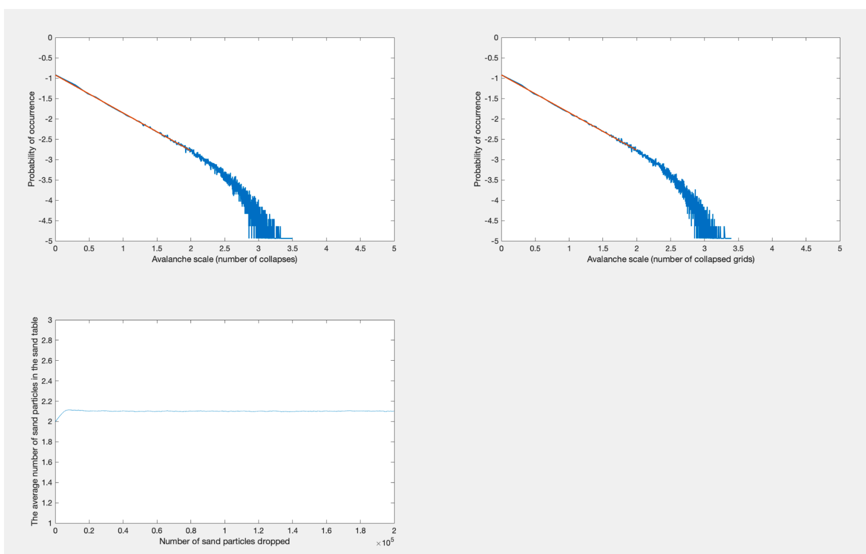

Figure 13. Avalanche size distributions for the mixed symmetric toppling rule (Scenario 2)

Scenario 3. The first asymmetric rule directs topples to neighbors at $\{(-1,1),(0,-1),(0,1),(1,1)\}$. This simulation yields a critical exponent of $\alpha \approx$ -1.31 for both avalanche size and area, as shown in Figure 14.

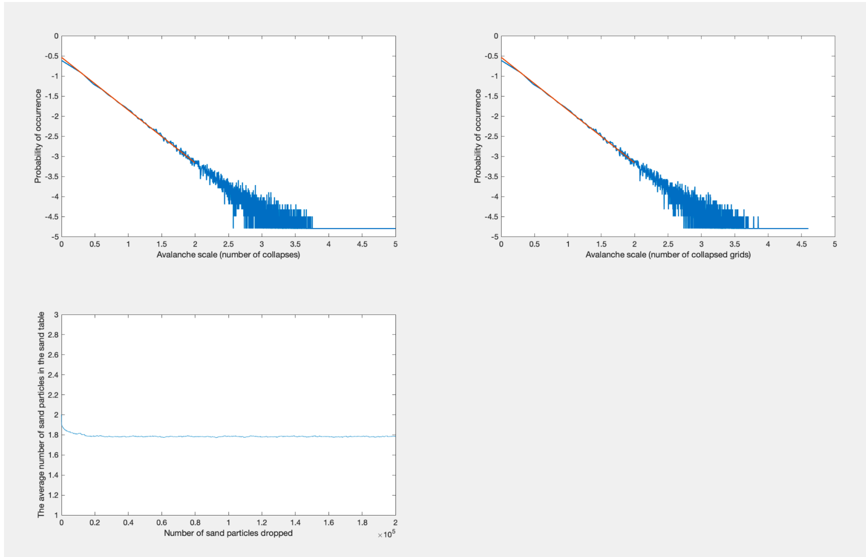

Figure 14. Avalanche size distributions for the first asymmetric toppling rule (Scenario 3)

Scenario 4. The second asymmetric rule directs topples to neighbors at $\{(-1,-1),(-1,1),(0,-1),(0,1)\}$. This model results in a critical exponent of $\alpha \approx$ -1.34 for both metrics, as shown in Figure 15.

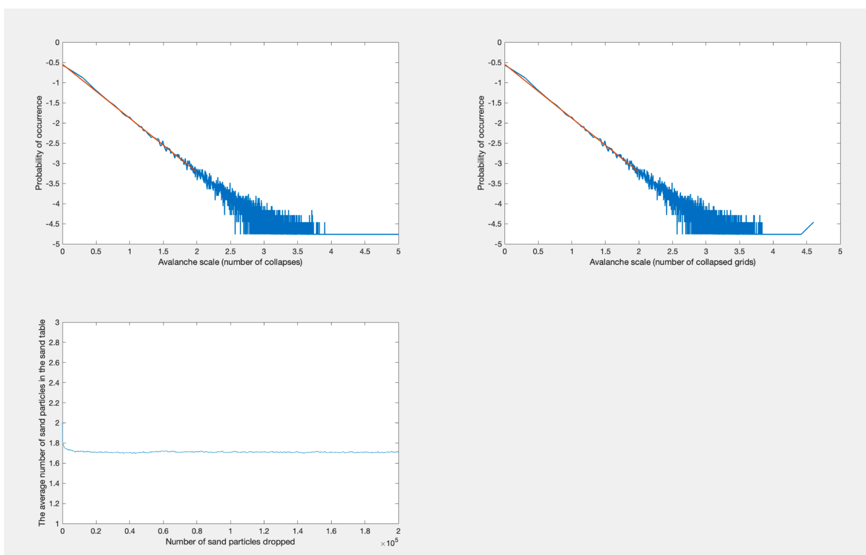

Figure 15. Avalanche size distributions for the second asymmetric toppling rule (Scenario 4)

The results of the four scenarios for fixed toppling structures under periodic boundary conditions, confirm the findings from the open boundary experiments. The symmetric toppling rules produce critical exponents close to -0.93, while the asymmetric rules yield significantly different exponents averaging -1.33. This reinforces the conclusion that breaking the spatial symmetry of the toppling rule is sufficient to move the system into a new universality class.

4.1.2. Randomized toppling structures

We next implemented the randomized toppling structures with periodic boundary conditions to see if the previous findings hold.

Random-Fixed Structure. In the model with quenched disorder, each site is assigned a fixed but random set of four neighbors from its Moore neighborhood. A single realization (Figure 16) yields exponents of $\alpha \approx -1.10$ (size) and $ $\alpha \approx -1.07$ (area). Averaging over ten independent network realizations confirms these values (Figure 17).

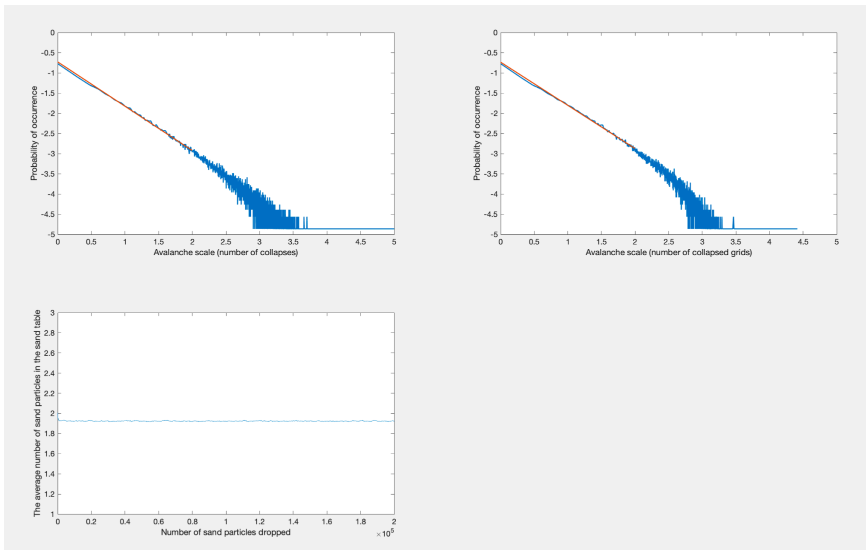

Figure 16. Avalanche size distributions for a single realization of the random-fixed structure model

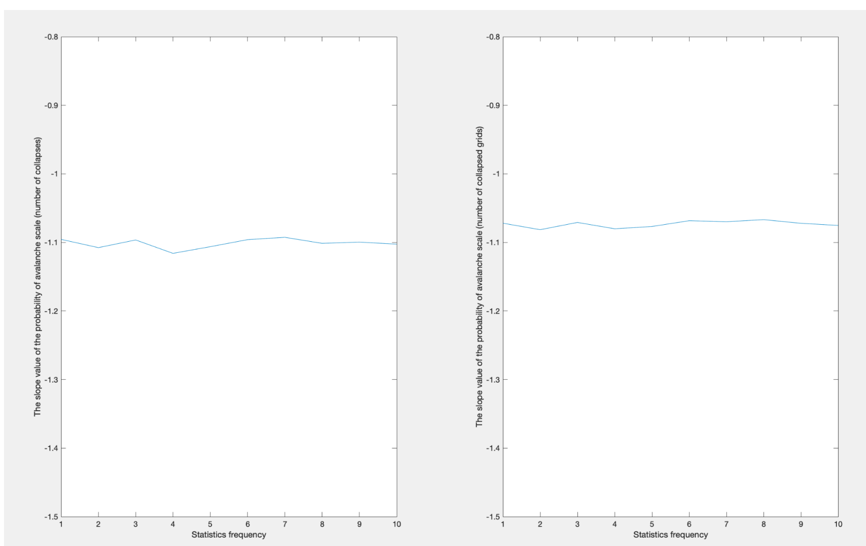

Figure 17. Critical exponents measured across ten different realizations of the random-fixed model

Random Structure. Finally, the dynamic random model, where the toppling neighborhood is chosen anew for each toppling event, was simulated. This model (Figure 18) yields exponents of $\alpha \approx -1.09$ for avalanche size and $\alpha \approx -1.07$ for the avalanche area. These values are consistent with the random-fixed case and, as with the open boundary condition, fall between the exponents of the purely symmetric and asymmetric fixed structures.

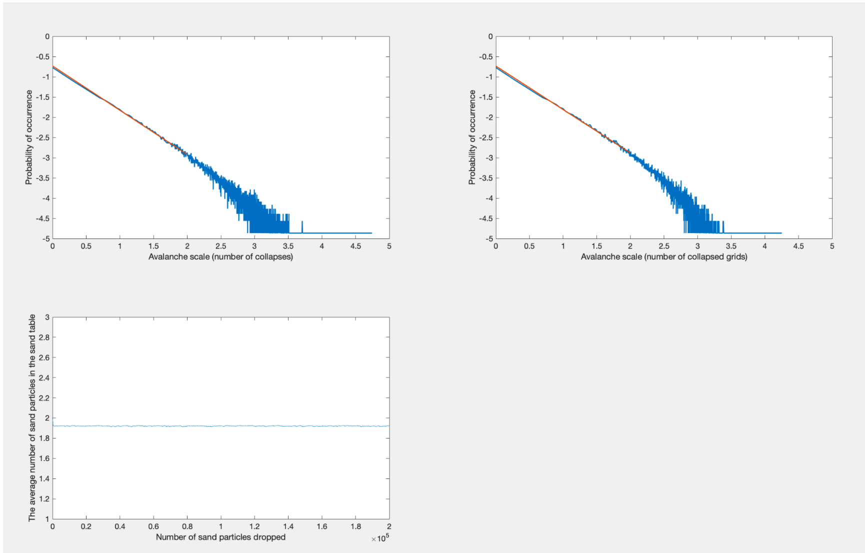

Figure 18. Avalanche size distributions for the dynamic random structure model under periodic boundary conditions

4.2. Influence of interaction range: varying neighborhood size

To bridge the gap between purely local interactions and long-range connections, we investigated how the system's critical behavior changes as the toppling neighborhood is gradually expanded. In this model, an unstable site distributes four grains to four sites chosen uniformly at random from a surrounding square Moore neighborhood of linear size k . The general rule is:

$$If z(x_i, y_i) \geq 4 \begin{cases} z(x_i, y_i) \rightarrow z(x_i, y_i) - 4 \\ z(x\prime, y\prime) \rightarrow z(x\prime, y\prime) + 1 \\ for 4 random sites (x\prime, y\prime) \in N_k(i,j) \end{cases} \tag{15}$$

where $N_k(i,j)$ is the set of sites in the $k \times k$ area centered on (x_i, y_i) . We highlight two illustrative cases below.

Short-Range Interaction (2×2 Neighborhood)

For $k = 2$, the interaction range is slightly larger than the nearest-neighbor case. The model yields a critical exponent of α ≈ -1.25 for avalanche size and α ≈ -1.23 for the avalanche area, as shown in Figure 19.

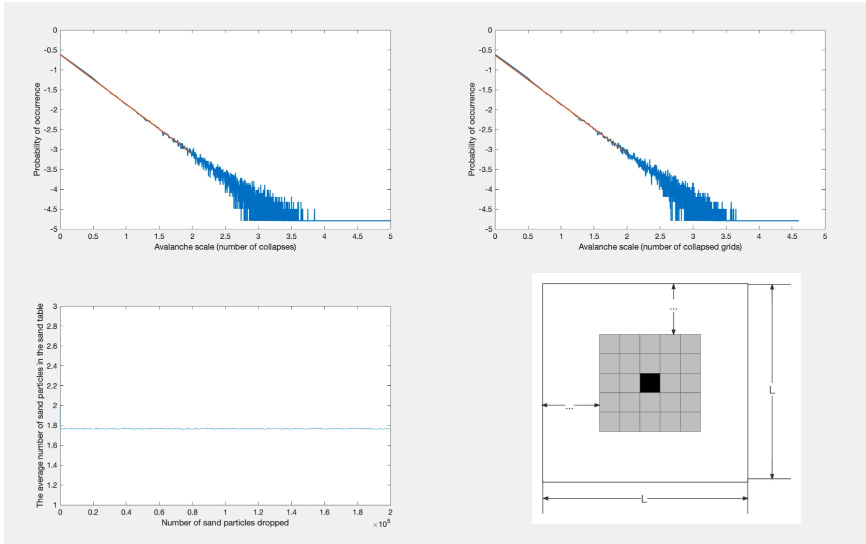

Figure 19. Schematic and avalanche distribution for the 2×2 toppling neighborhood

Long-Range Interaction (100×100 Neighborhood)

For $k = 100$, the neighborhood covers a quarter of the 200×200 lattice, making the interaction effectively long-range. This model produces a critical exponent of $\alpha \approx$ -1.47 for both metrics, as shown in Figure 20.

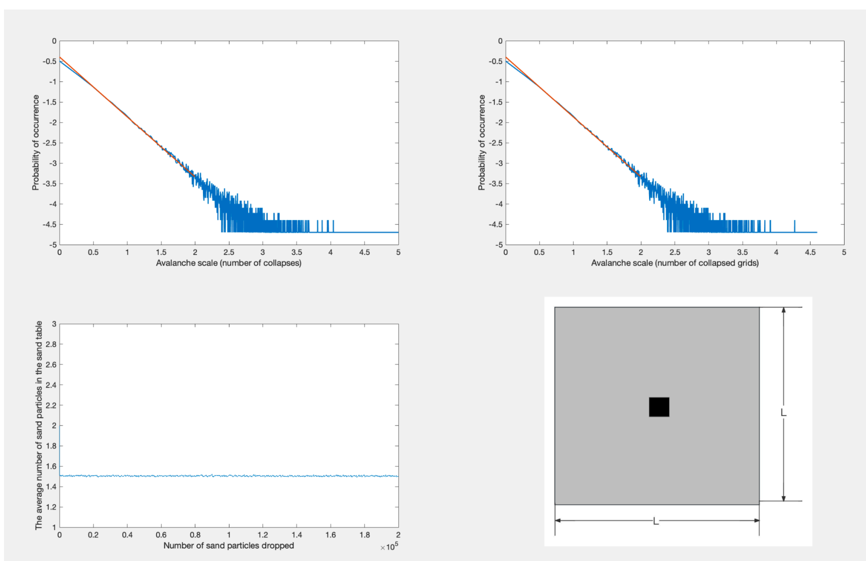

Figure 20. Schematic and avalanche distribution for the 100×100 toppling neighborhood

Crossover Behavior

To map the full crossover between these regimes, we varied the neighborhood size k from 2 to 100. The resulting critical exponents are plotted in Figure 21. The plot clearly shows a monotonic transition in the system's behavior. As the interaction range increases, the critical exponent shifts smoothly from approximately -1.2 towards -1.5. This demonstrates that the universality class of the system is not fixed but changes with the spatial scale of the interactions, interpolating between a local and a mean-field-like regime.

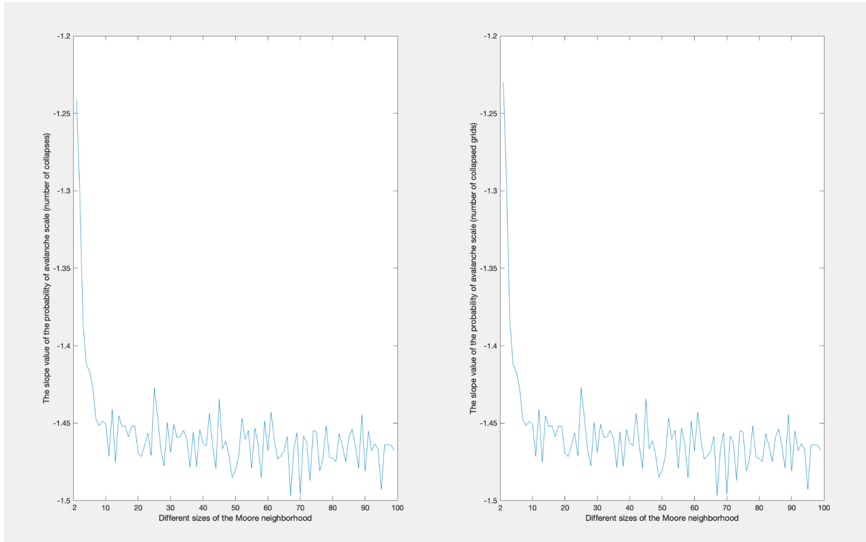

Figure 21. Critical exponent as a function of the toppling neighborhood size *k*

4.3. Influence of long-range connections

To directly probe the impact of non-local interactions, we modified the canonical four-neighbor BTW model by replacing a number of its local connections with long-range ones. In this model, an unstable site topples by distributing n_{LR} grains to randomly chosen sites across the entire lattice, while the remaining $4 - n_{LR}$ grains are sent to unique, randomly chosen nearest neighbors. All simulations were performed under periodic boundary conditions with the standard dissipation mechanism.

4.3.1. Varying the number of long-range connections

We systematically increased the number of long-range connections, n_{LR}, from one to four.

One Long-Range Connection ($n_{LR} = 1$). When one of the four connections is long-range, the model yields a critical exponent of α ≈ -1.41 for both avalanche size and area, as shown in Figure 22.

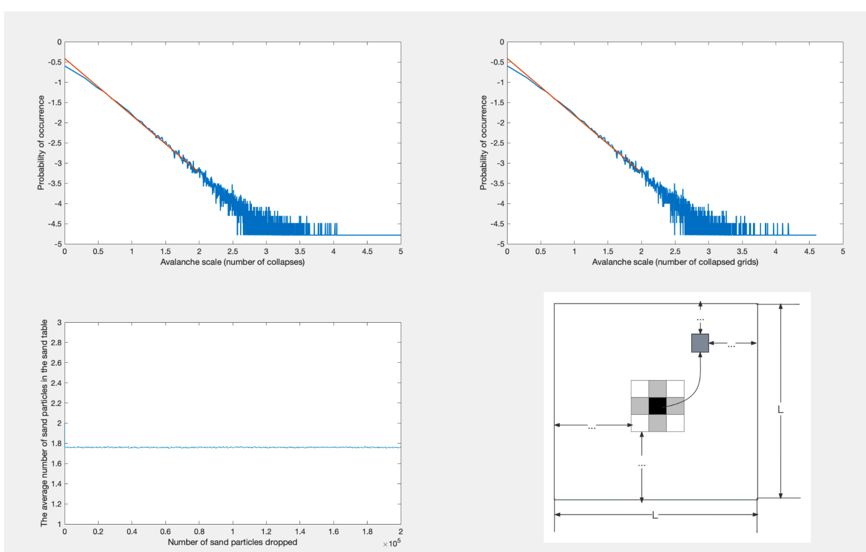

Figure 22. Results for a model with one long-range and three local connections

Due to space constraints, we omit the detailed results for other cases and present the results in Table 1, which reveals a crucial finding: the introduction of even a single long-range connection is sufficient to shift the critical exponent from the BTW value of ≈ -1.0 to a value of ≈ -1.4. Increasing the number of long-range connections further deepens this shift, but the majority of the change occurs with the first non-local link. This strongly suggests that any amount of non-locality rapidly drives the system into a mean-field universality class, characterized by an exponent of ≈ -1.5.

Table 1. Critical exponents (α) for models with a varying number of long-range connections

Metric	$n_{LR} = 1$	$n_{LR} = 2$	$n_{LR} = 3$	$n_{LR} = 4$
Avalanche Size	-1.41	-1.45	-1.46	-1.48
Avalanche Area	-1.41	-1.45	-1.46	-1.48

4.3.2. Crossover from local to long-range dynamics

To visualize the transition between the local and long-range universality classes, we designed a hybrid model. At each toppling event, a choice is made with probability p_{LR} to use a toppling rule with one long-range connection. With probability $1 - p_{LR}$, the purely local four-neighbor BTW rule is used. We then measured the system's effective critical exponent as a function of p_{LR}.

As shown in Figure 23, the critical exponent interpolates smoothly between the two limiting values. As the probability of a long-range topple increases from 0 to 1, the exponent transitions from α ≈ -1.0 to α ≈ -1.5. This result provides a clear picture of the crossover and demonstrates that the macroscopic critical behavior of the system can be tuned by altering the microscopic probability of non-local interactions.

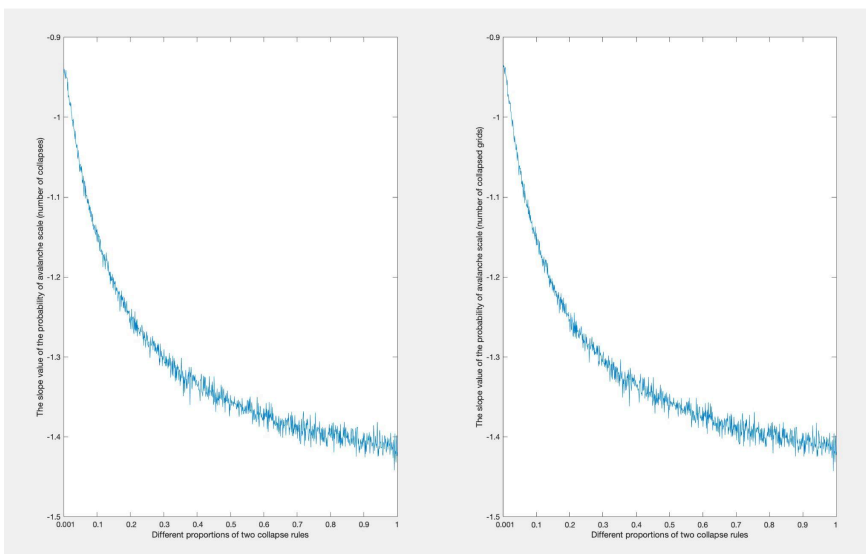

Figure 23. Crossover of the critical exponent as a function of the probability of a long-range topple, p_{LR}

5. Discussion

In this study, we systematically investigated how relaxing the assumptions of local, symmetric interactions affects the self-organized critical behavior of the sandpile model. Our numerical simulations reveal two primary findings: first, that breaking the spatial symmetry of the toppling rule is sufficient to shift the critical exponent of the avalanche size distribution from the canonical BTW value of α ≈ -1.0 to a new value of α ≈

-1.3. Second, and more significantly, the introduction of even a single long-range connection rapidly drives the system into a different universality class characterized by an exponent of $\alpha \approx$ -1.5, which is consistent with mean-field behavior.

5.1. Implications for real-world complex systems

These findings have profound implications for the application of SOC models to natural and technological systems, where interactions are rarely confined to immediate neighbors. For example:

• In forest fire dynamics, while fires often spread locally to adjacent trees, embers carried by wind can spark new fires at great distances. Our results suggest that this non-local mechanism is not just a minor correction but a critical feature that can fundamentally alter the statistics of fire sizes, pushing the system into a mean-field regime.

• In neuroscience, the brain's structure is a quintessential example of a network with both local connections (between nearby neurons) and long-range shortcuts (via axons connecting distant brain regions). Our model supports the idea that these long-range connections are crucial for the brain's complex, system-wide dynamics and that purely local models may fail to capture the correct statistics of neural avalanches.

• In transportation and infrastructure networks, a local traffic jam on a city street can have cascading effects on nearby intersections (local interaction), but an accident on a major highway can create disruptions miles away almost instantly (long-range connection) [17, 18]. The observed shift in the critical exponent underscores how vulnerable such systems are to non-local failures.

In all these cases, our work suggests that the network topology is a dominant factor in shaping the macroscopic critical behavior. Models that neglect non-local or asymmetric interactions may fail to accurately predict the frequency and scale of cascading events in the real world.

5.2. Limitations and future directions

While this study provides clear evidence for the importance of network topology, our model remains a simplified abstraction. The connections in our long-range models were chosen uniformly at random, whereas the connections in many real-world networks follow more complex distributions (e.g., small-world or scale-free).

This points to several exciting avenues for future research. An immediate next step would be to implement the sandpile model on more realistic network topologies. Furthermore, exploring the interplay between spatial asymmetry and long-range connections could reveal more nuanced critical behaviors. These investigations would help bridge the gap between abstract SOC models and the intricate, non-local dynamics of the complex systems they aim to describe, laying a foundation for a deeper understanding of stochastic processes on complex networks.

6. Conclusion

We have demonstrated that the universality class of the BTW sandpile model is not robust against changes to its underlying interaction topology. By introducing spatial asymmetry in the local toppling rules or by adding non-local shortcuts, the system's critical behavior is qualitatively altered. Breaking symmetry shifts the critical exponent to $\alpha \approx$ -1.3, while introducing even a sparse number of long-range connections drives the exponent to the mean-field value of $\alpha \approx$ -1.5. These results highlight the critical role that network structure plays in self-organizing systems and have significant implications for modeling a wide range of real-world phenomena.

References

[1] Bak, P., Tang, C., & Wiesenfeld, K. (1987). Self-organized criticality: An explanation of the 1/f noise. *Physical review letters, 59*(4), 381.

[2] Juanico, D. E., Longjas, A., Batac, R., & Monterola, C. (2008). Avalanche statistics of driven granular slides in a miniature mound. *Geophysical Research Letters, 35*(19), L19403.

[3] Zeng, H. L., Zhu, C. P., Wang, S. X., Guo, Y. D., Gu, Z. M., & Hu, C. K. (2020). Scaling behaviors and self-organized criticality of two-dimensional small-world neural networks. *Physica A: Statistical Mechanics and its Applications, 540*, 123191.

[4] Piegari, E., Cataudella, V., Di Maio, R., Milano, L., & Nicodemi, M. (2006). A cellular automaton for the factor of safety field in landslides modeling. *Geophysical Research Letters, 33*(1), L01403.

[5] Lübeck, S., & Usadel, K. D. (1993). SOC in a class of sandpile models with stochastic dynamics. *Fractals, 1*(4), 1030-1036.

[6] Majumdar, S. N., & Dhar, D. (1991). Height correlations in the Abelian sandpile model. *Journal of Physics A: Mathematical and General, 24*(7), L357.

[7] Chhajed, K. (2020). *Stochastic Sandpile Models in two Dimensions* [Doctoral dissertation, Indian Institute of Science Education and Research Mohali].

[8] Hao, L., Yu, X., Zhang, T., & Schulzrinne, H. (2022). Distributed MQTT Brokers at Network Edges: A Study on Message Dissemination. In *2022 IEEE International Conferences on Internet of Things (iThings)* (pp. 17-24).

[9] Hao, L., Naik, V., & Schulzrinne, H. (2022). DBAC: Directory-based access control for geographically distributed IoT systems. In *IEEE Conference on Computer Communications* (pp. 360-369).

[10] Falk, J., Winkler, M., & Kinzel, W. (2015). On the effect of the drive on self-organized criticality. *Journal of Physics A: Mathematical and Theoretical, 48*(40), 405003.

[11] Manna, S. S., & Giri, D. (1997). Sandpile model with activity inhibition. *Physical Review E, 56*(5), R4914.

[12] Yadav, A. C., Quadir, A., & Jafri, H. H. (2022). Finite-size scaling of critical avalanches. *Physical Review E, 106*(1), 014148.

[13] Lee, Y. T., Chen, C. C., Lin, C. Y., & Chuang, Y. T. (2014). Quasi-periodicity of large avalanches in the long-range connective sandpile models and its implication in natural earthquakes. *Europhysics Letters, 105*(4), 40003.

[14] Menchón, S. A., & Román, P. (2020). Emergence of power law distributions for odd and even lifetimes. *Physical Review E, 102*(6), 062143.

[15] Bak, P., & Tang, C. (1989). Earthquakes as a self-organized critical phenomenon. *Journal of Geophysical Research: Solid Earth, 94*(B11), 15635-15637.

[16] Badie-Modiri, A., Rizi, A. K., Karsai, M., & Kivelä, M. (2022). Directed percolation in temporal networks. *Physical Review Research, 4*(2), L022047.

[17] Huang, K., & Du, Q. (2022). Stability of a nonlocal traffic flow model for connected vehicles. *SIAM Journal on Applied Mathematics, 82*(1), 221-243.

[18] Hao, L., Jin, C., Gao, X., Kong, L., Wu, F., & Chen, G. (2017). QoE-aware optimization for SVC-based adaptive streaming in D2D communications. In *2017 IEEE 36th International Performance Computing and Communications Conference (IPCCC)* (pp. 1-8).